Electronic Supplementary Information

Modified Polydopamine Derivatives as High-Performance Organic Anode for Potassium-Ion Batteries

*Yi Zhang, Chenglin Zhang, Qun Fu, Huaping Zhao, and Yong Lei**

Y. Z., Q.F.

Institute of Nanochemistry and Nanobiology, School of Environmental and Chemical Engineering, Shanghai University, Shanghai 200444, China

C.L. Z., H.P. Z., Y. L.

Fachgebiet Angewandte Nanophysik, Institut für Physik & IMN MacroNano (ZIK), Technische Universität Ilmenau, Ilmenau 98693, Germany

E-mail: yong.lei@tu-ilmenau.de

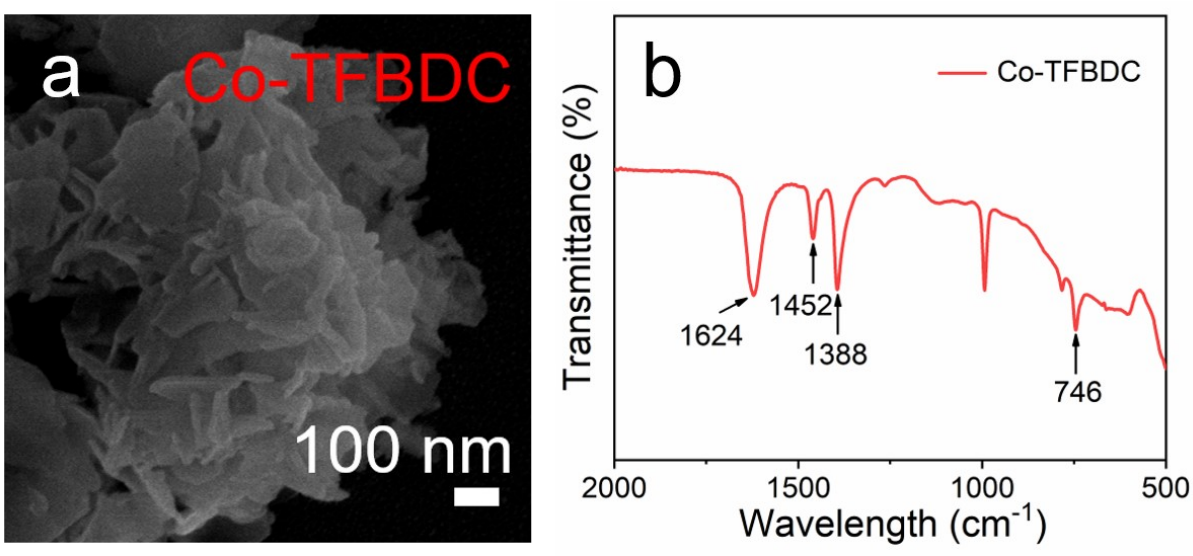

Figure S1. a) SEM image, and b) FTIR spectrum of the prepared Co-TFBDC.

According to the Figure S1a, the scanning electron microscopy (SEM) image presents the uniform nanosphere structure of prepared Co-TFBDC (< 1 um). Moreover, in the Fourier transform infrared spectroscopy (FTIR) spectrum of Co-TFBDC (Figure S1b), the peak at 1624 cm^{-1} is assigned to asymmetric stretching vibrations of -COO-, peaks at 1452 and 1388 cm^{-1} can be attributed to the symmetric stretching vibrations, and the peak at 746 cm^{-1} shows the out of plane vibration of 1,4-substituted benzene of the linker molecules (out of plane C-F bending modes). These results indicate that the urchin-like Co-TFBDC template has been successfully synthesized.

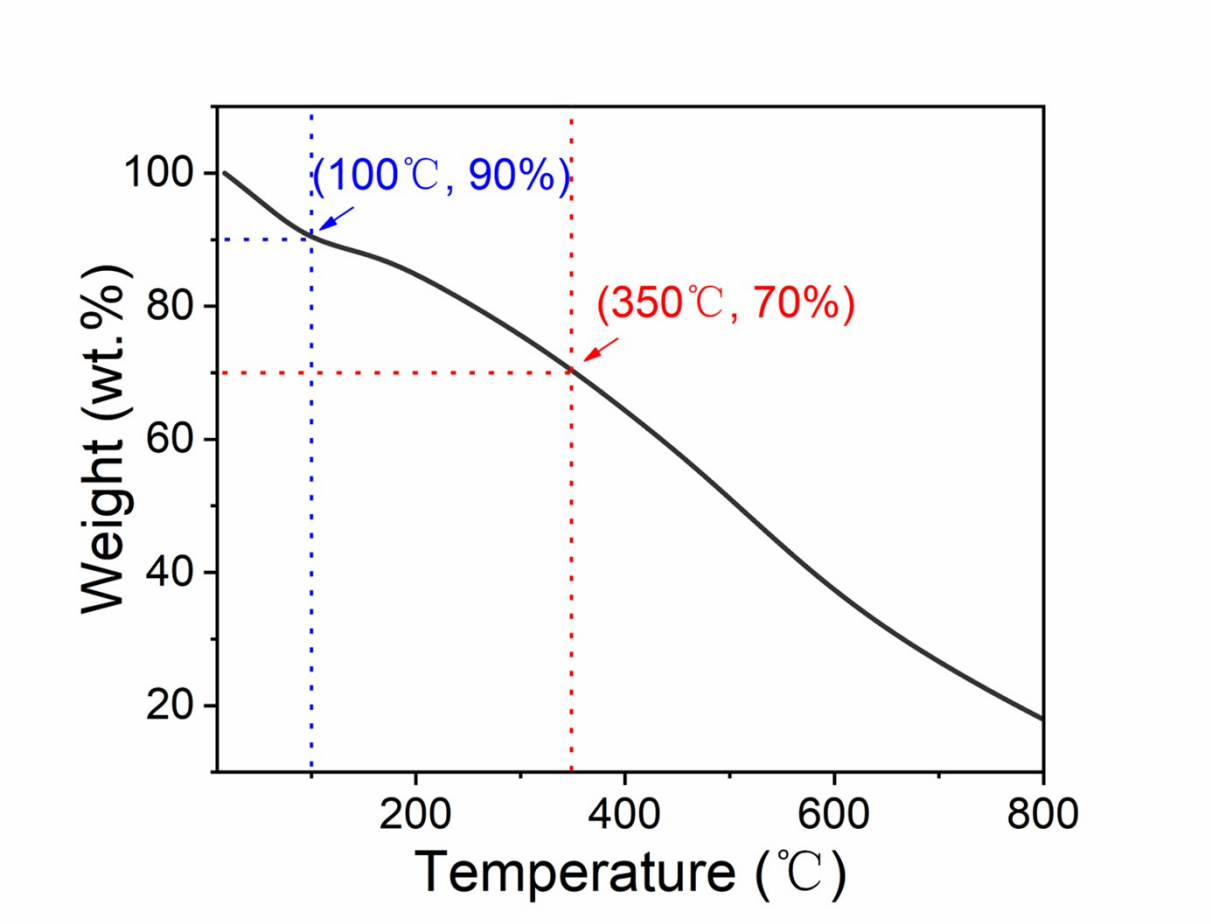

Figure S2. TG curve of MPDA at a heating rate of 10 ℃ min^{-1} under a N_2 atmosphere.

As shown in Figure S2, the thermogravimetric analysis (TGA) curve of MPDA can be divided into three parts based on the rate of weight loss: <100°C, 100–350°C, and >350°C, each of which corresponds to diverse changing process. When the temperature is less than 100°C, the mass change is due to the loss of water. Weight loss occurs due to cross-linking of polymer chains and conversion of functional groups at temperatures ranging from 100 to 350°C. When the temperature rises above 350°C, carbonization begins, resulting in rapid weight loss. According to the TGA result, we set a series of annealing temperatures for comparison (150℃, 350℃, and 550℃). Then the MPDA-150, MPDA-350, and MPDA-550 materials were obtained by annealing MPDA at 150℃, 350℃, and 550℃ in a N_2 atmosphere, respectively.

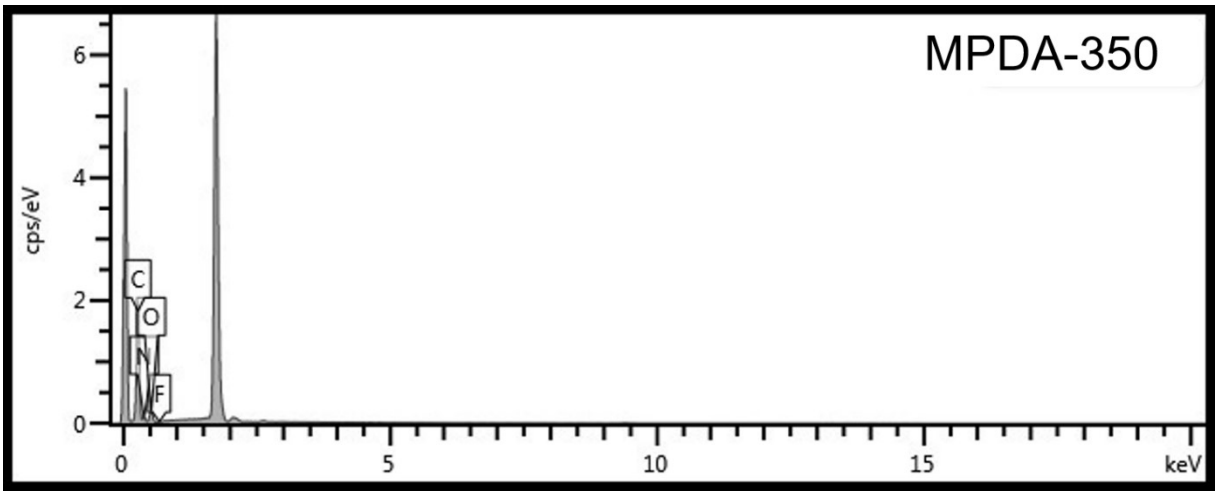

Figure S3. EDS spectrum of MPDA-350.

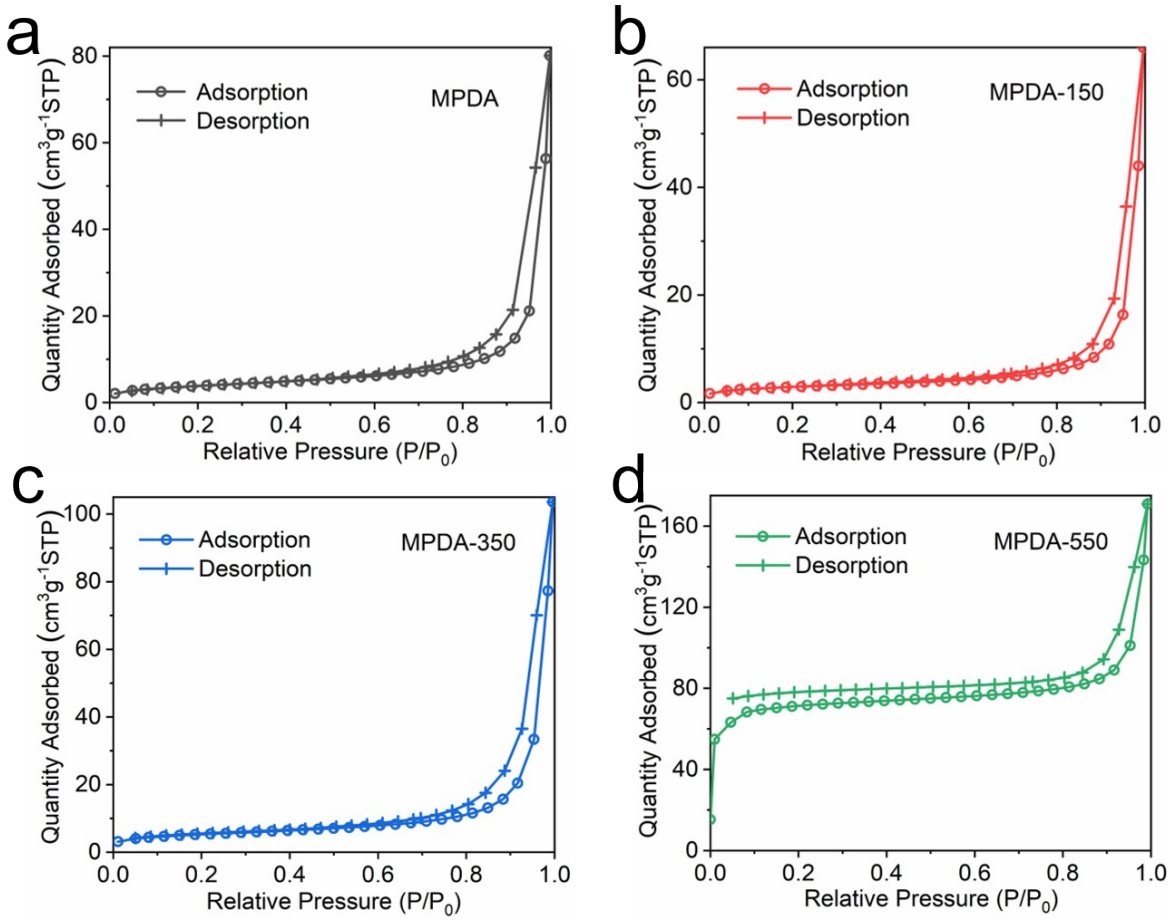

Figure S4. Nitrogen adsorption-desorption isotherms of a) MPDA, b) MPDA-150, c) MPDA-350, and d) MPDA-550.

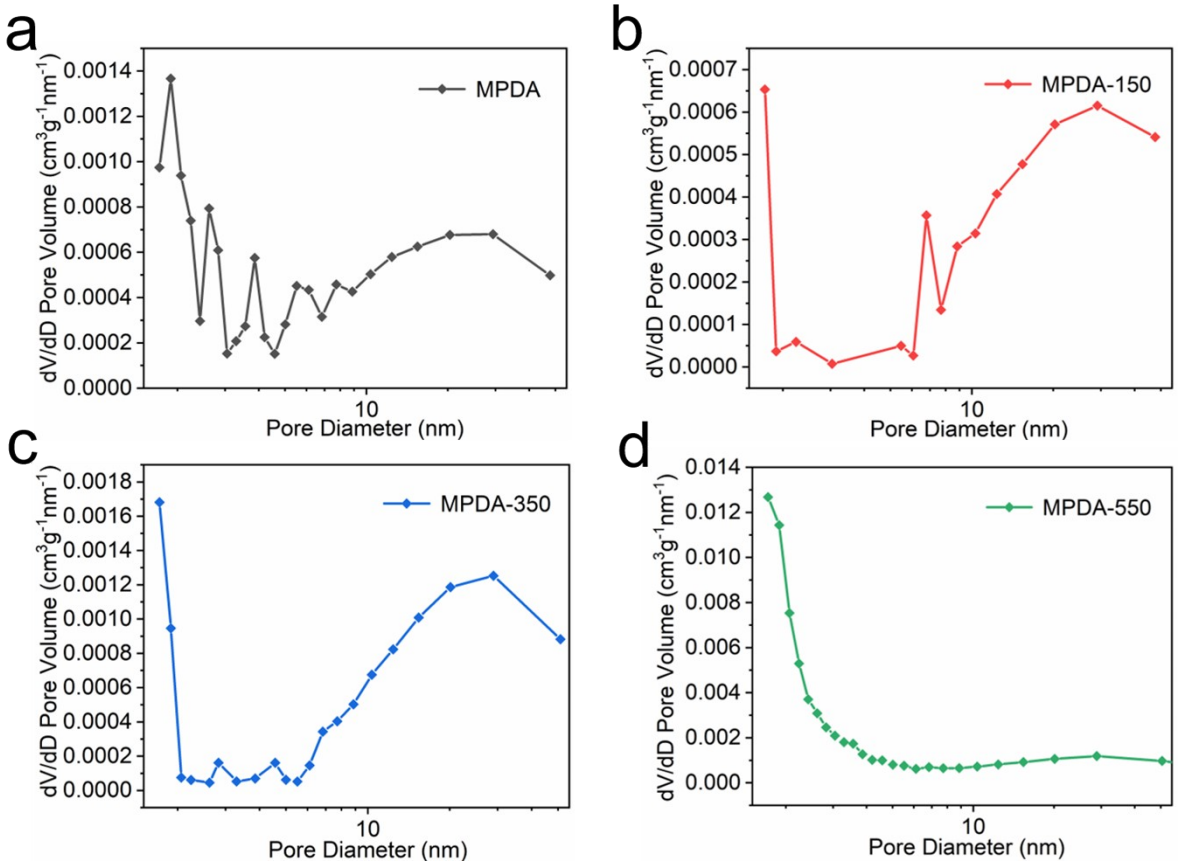

Figure S5. Pore size distribution of a) MPDA, b) MPDA-150, c) MPDA-350, and d) MPDA-550.

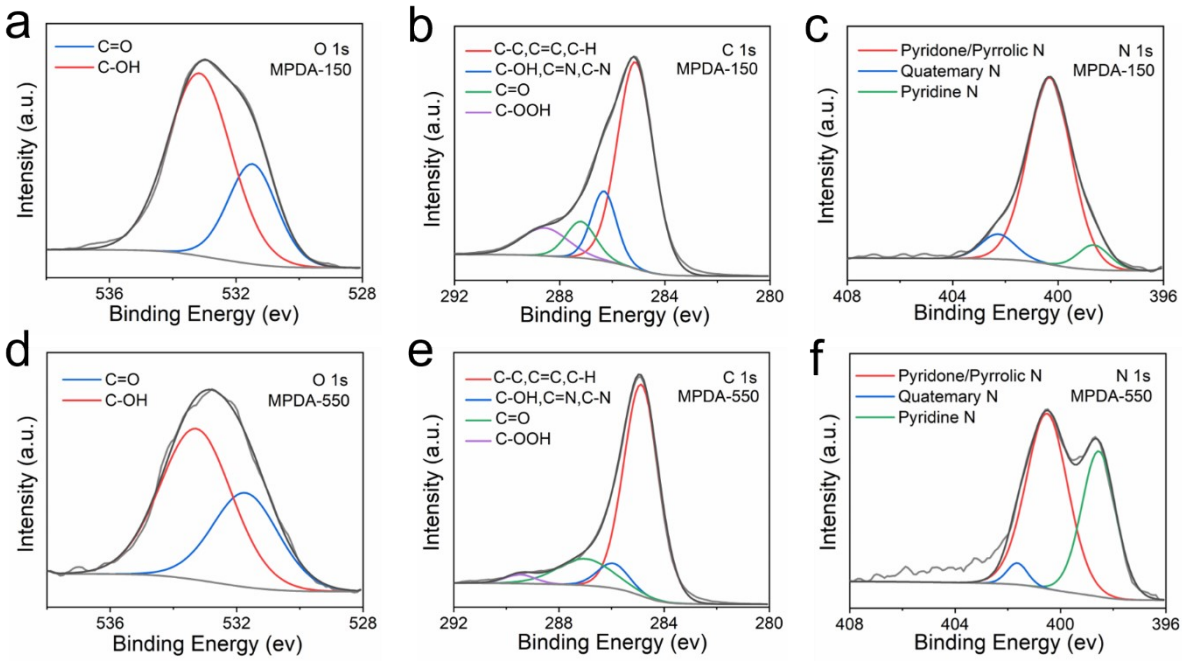

Figure S6. HR-XPS spectra of O 1s, C 1s and N 1s peak fittings of a-c) MPDA-150, d-f) MPDA-550.

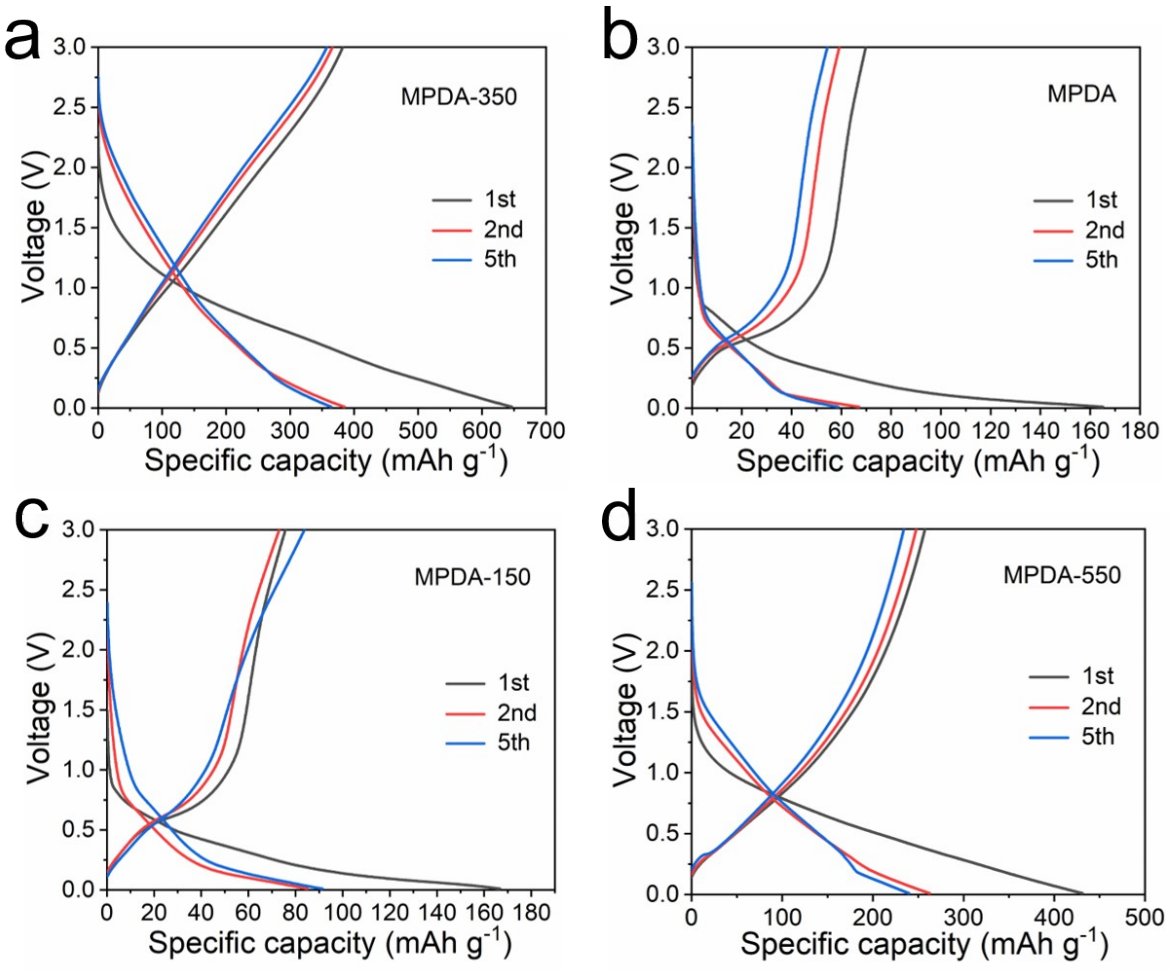

Figure S7. Charge/discharge profiles of a) MPDA-350, b) MPDA, c) MPDA-150, and d) MPDA-550 at 100 mA g^{-1}.

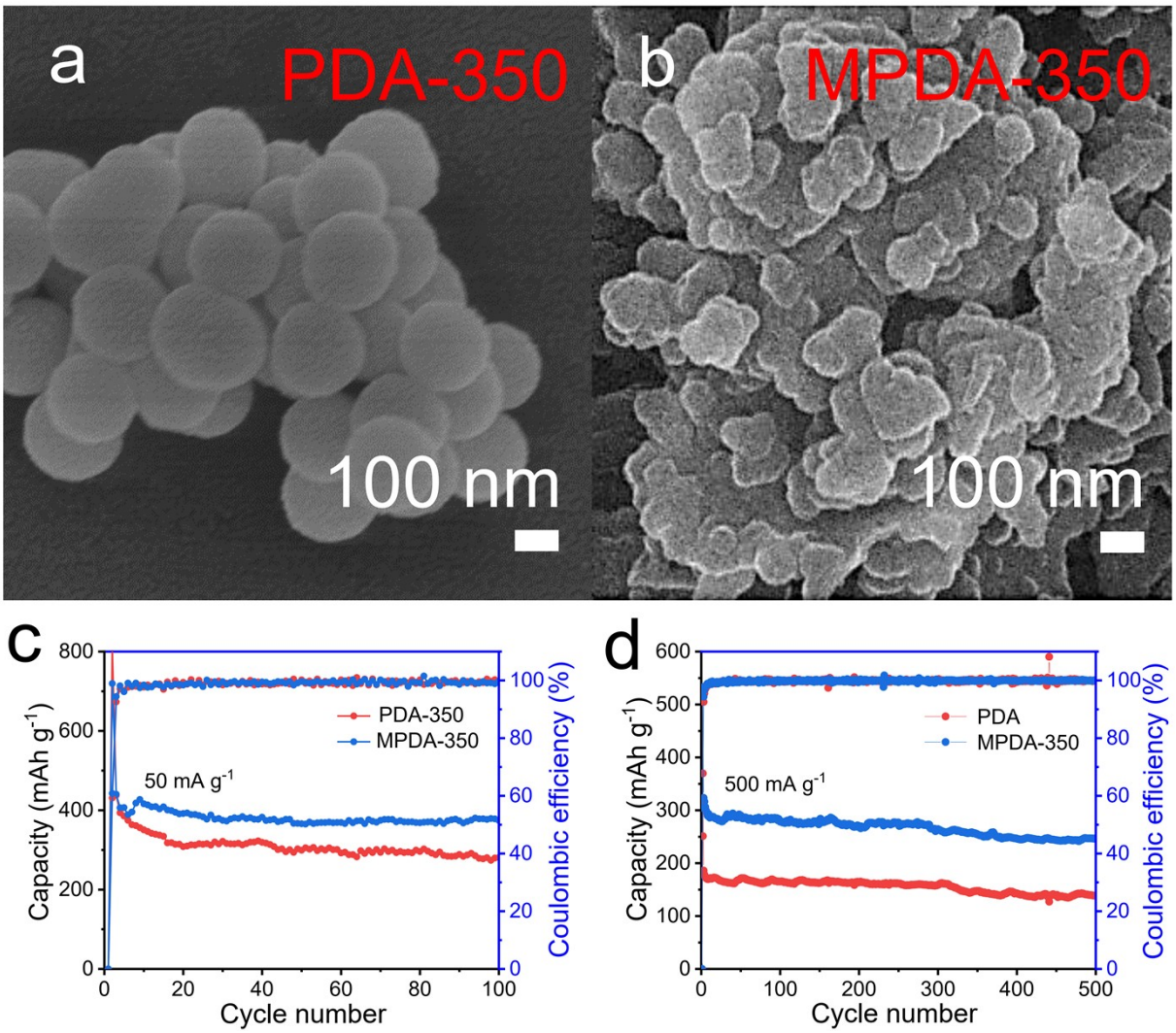

Figure S8. SEM images of a) PDA-350 and b) MPDA-350. Cycling performance at c) 50 mA g^{-1} and d) 500 mA g^{-1} of PDA-350 and MPDA-350.

Table S1. Comparison of some representative anodes of half-cell PIBs.

Materials	Initial discharge /charge Capacity (mAh g^{-1})	Rate ability (mAh g^{-1})	Cyclability (mAh g^{-1})	Ref.
MPDA-350	646.4/382.3 at 100 mA g^{-1}	403.2 at 50 mA g^{-1}; 209.6 at 5000 mA g^{-1}	246.8 after 500 cycles at 500 mA g^{-1}	This work
VK@GNT	466/338.9 at 100 mA g^{-1}	203 at 200 mA g^{-1}; 165 at 1000 mA g^{-1}	222.3 after 100 cycles at 100 mA g^{-1}	SR1
H_2TP	/	240 at 50 mA g^{-1}; 56 at 400 mA g^{-1}	240 after 150 cycles at 50 mA g^{-1}	SR2
K_4PTC@CNT	417/137 at 50 mA g^{-1}	107 at 100 mA g^{-1}; 78 at 500 mA g^{-1}	97 after 500 cycles at 50 mA g^{-1}	SR3
PyBT	358 at 30 mA g^{-1}	428 at 30 mA g^{-1}	272 after 500 cycles at 50 mA g^{-1}	SR4
K_2BPDC	/	105 at 50 mA g^{-1}; 52 at 500 mA g^{-1}	75 after 3000 cycles at 1000 mA g^{-1}	SR5
NCNTs	1215.7/297.2 at 50 mA g^{-1}	293.1 at 50 mA g^{-1}; 131 at 2000 mA g^{-1}	257 after 300 cycles at 50 mA g^{-1}	SR6
HCONs-500	926/326 at 100 mA g^{-1}	311 at 100 mA g^{-1}; 105 at 10000 mA g^{-1}	132 after 5000 cycles at 2000 mA g^{-1}	SR7
OFPCN	405 at 100 mA g^{-1}	481 at 50 mA g^{-1}; 78 at 20000 mA g^{-1}	111 after 5000 cycles at 10000 mA g^{-1}	SR8
Sn_4P_3/C	588.7 at 50 mA g^{-1}	399.4 at 50 mA g^{-1}; 221.9 at 1000 mA g^{-1}	307.2 after 50 cycles at 50 mA g^{-1}	SR9
SSFG	450 at 500 mA g^{-1}	319 at 200 mA g^{-1}; 135 at 2000 mA g^{-1}	234 after 280 cycles at 500 mA g^{-1}	SR10

References:

SR1 Q. Xue, D. N. Li, Y. X. Huang, X. X. Zhang, Y. S. Ye, E. S. Fan, L. Li, F. Wu and R. J. Chen, *J. Mater. Chem. A.*, 2018, **6**, 12559-12564.

SR2 C. Wang, W. Tang, Z. Y. Yao, Y. Z. Chen, J. F. Pei and C. Fan, *Org. Electron.*, 2018, **62**, 536-541.

SR3 C. Wang, W. Tang, Z. Y. Yao, B. Cao and C. Fan, *Chem. Commun.*, 2019, **55**, 1801-1804.

SR4 C. Zhang, Y. Qao, P. X. Xiong, W. Y. Ma, P. X. Bai, X. Wang, Q. Li, J. Zhao, Y. F. Xu, Y. Chen, J. H. Zeng, F. Wang, Y. H. Xu and J. X. Jiang, *ACS Nano.*, 2019, **13**, 745-754.

SR5 C. Li, Q. J. Deng, H. C. Tan, C. Wane, C. Fan, J. F. Pei, B. Cao, Z. H. Wang and J. Z. Li, *ACS Applied Materials & Interfaces*, 2017, **9**, 27414-27420.

SR6 P. X. Xiong, X. X. Zhao and Y. H. Xu, *Chem. Sus. Chem.*, 2018, **11**, 202-208.

SR7 S. T. Liu, B. B. Yang, J. S. Zhou and H. H. Song, *J. Mater. Chem. A.*, 2019, **7**, 18499-18509.

SR8 J. Lu, C. L. Wang, H. L. Yu, S. P. Gong, G. L. Xia, P. Jiang, P. P. Xu, K. Yang and Q. W. Chen, *Adv. Funct. Mater.*, 2019, **29**, 1906126.

SR9 W. C. Zhang, J. F. Mao, S. A. Li, Z. X. Chen and Z. P. Guo, *J. Am. Chem. Soc.*, 2017, **139**, 3316-3319.

SR10 J. W. Wang, M. Y. Cao, F. Xu, X. L. Zhu, K. Rashid, Y. Wang and L. Huang, *New J. Chem.*, 2021, **45**, 993-1000.